International Journal of Earth, Energy and Environmental Sciences
ISSN: 2517-942X
Vol:9, No:12, 2015

Simulating the Interaction between Groundwater and Brittle Failure in Open Pit Slopes

Janisse Vivas, Doug Stead, Davide Elmo, Charles Hunt

***Abstract*—**This paper presents the results of a study on the influence of varying percentages of rock bridges along a basal surface defining a biplanar failure mode. A pseudo-coupled-hydromechanical brittle fracture analysis is adopted using the state-of-the-art code Slope Model. Model results show that rock bridge failure is strongly influenced by the incorporation of groundwater pressures. The models show that groundwater pressure can promote total failure of a 5% rock bridge along the basal surface. Once the percentage of the rock bridges increases to 10 and 15%, although, the rock bridges are broken, full interconnection of the surface defining the basal surface of the biplanar mode does not occur. Increased damage is caused when the rock bridge is located at the daylighting end of the basal surface in proximity to the blast damage zone. As expected, some cracking damage is experienced in the blast damage zone, where properties representing a good quality controlled damage blast technique were assumed. Model results indicate the potential increase of permeability towards the blast damage zone.

***Keywords*—**Slope model, lattice spring, blasting damage zone.

I. Introduction

IN open pit mining, groundwater flow usually takes place along discontinuities within the pit slope. Water pressure acting in pore spaces, fractures or other discontinuities in the rock mass present in the pit slope will reduce the rock mass and discontinuity strength, and may therefore have a large influence on the performance, safety, and economics of a mining operation [1].

A reduction in pore pressure within a pit slope may occur as a result of different processes including:

1) Groundwater flowing away from a particular zone due to seepage forces.
2) Increase in the total porosity as a result of lithostatic unloading and relaxation.
3) Increase in total porosity as a result of drainage or removal of water from the overlying rock.

In open pit mining environments, changes in pore pressure usually occur as a result of groundwater flow [2]. Consequently, pore pressure is distributed through the whole mass, and not only restricted to the major geological structures.

Deformation as a result of unloading (excavation), leads to changes in the stresses and consequent changes in the pore fluid pressure. Additionally, pit excavation reduces the lateral and vertical stress resulting in strains that generally increase porosity, aperture, and connectivity between fractures [3].

At greater depths within the slope (>300m), the pre-existing deformation is smaller and the fracture porosity is comparatively high [4]. Further mining processes induce slope deformation and cause an increase in the porosity. Rock mass unloading occurs as a result of the stress field created by mining operations and often causes an opening or widening of fractures in the zone of relaxation around the mine excavation [5]. Hence, the magnitude of pore pressure dissipation, in response to material unloading, is more pronounced with depth [3], [4].

The development of the blast-damaged zone (over-break) is also important for pore pressure control. The blast-damage zone represents the area where properties and conditions are altered because of the excavation process. This zone is characterized by an area of reduced fluid pressure extending in all directions away from the zone. However, the shape and extent of the damage zone depends on many factors, including blasting procedures and rock properties, which vary considerably [4], [6]. The blast-induced damaged zone is comprised of macro to micro-cracks of various sizes, lengths, and shapes, with numerous rock bridges in between. Robertson [7] concluded that the rock bridges must fail in tension before global rock mass failure can occur. This complex crack pattern can affect the strength characteristics and thus influence the overall mechanical response of open pit slopes. Diederichs et al. [8] demonstrated the significance of the tensile strength of rock bridges under low confinement or distressed conditions. According to [9], the tensile strength will be very sensitive and important in the mechanical response of the blast-induced damaged rock mass around underground excavations. Additionally, the presence of groundwater in mining operations often creates significant geotechnical problems; most important being a reduction in stability of the pit slopes. Overall, reduction of pit slope stability can be due to pore water pressures and hydrodynamic shock due to blasting, which reduces the shear strength and can also reduce seepage pressures [10].

A. Groundwater Flow in Fractured Rock

Geological structure is a major contributor to the distribution and alignment of fractures in most mine settings. In hard rock lithologies, the first-order fracture sets are related to the main (primary) zones, and the rock's overall permeability is mostly controlled by the degree of interconnection of the first-order fractures with second, third and consecutive fractures [10].

Janisse Vivas and Charles Hunt are with Tetra Tech EBA, Vancouver, Canada (e-mail: Janisse.VivasBecerra@tetratech.com, Charles.Hunt@tetratech.com).

Doug Stead is with Simon Fraser University, Vancouver, BC, Canada (e-mail: dstead@sfu,ca).

Davide Elmo is with University of British Columbia, BC, Canada (e-mail: Davide_Elmo@golder.com).

Fig. 1 shows a typical fracture network comprising a few highly transmissive and pervasive "first order fractures" (A), a moderately transmissive second-order fracture (B) a lesser transmissive third-order fracture (C) and a low transmissive fourth-order fracture (D). This concept is known as the "A-B-C-D" concept of fracture flow [11]. The more permeable "A" fractures respond first to depressurisation by drainage, interconnectivity of these fractures allows rapid propagation of pressure changes throughout the system. As pressures within the first-order fractures begin to decrease, flow along the less permeable second-order fracture sets begin to occur towards the first-order fractures. This dual porosity response also occurs from third-order into second-order fractures, and so on through the entire interconnected network of fractures.

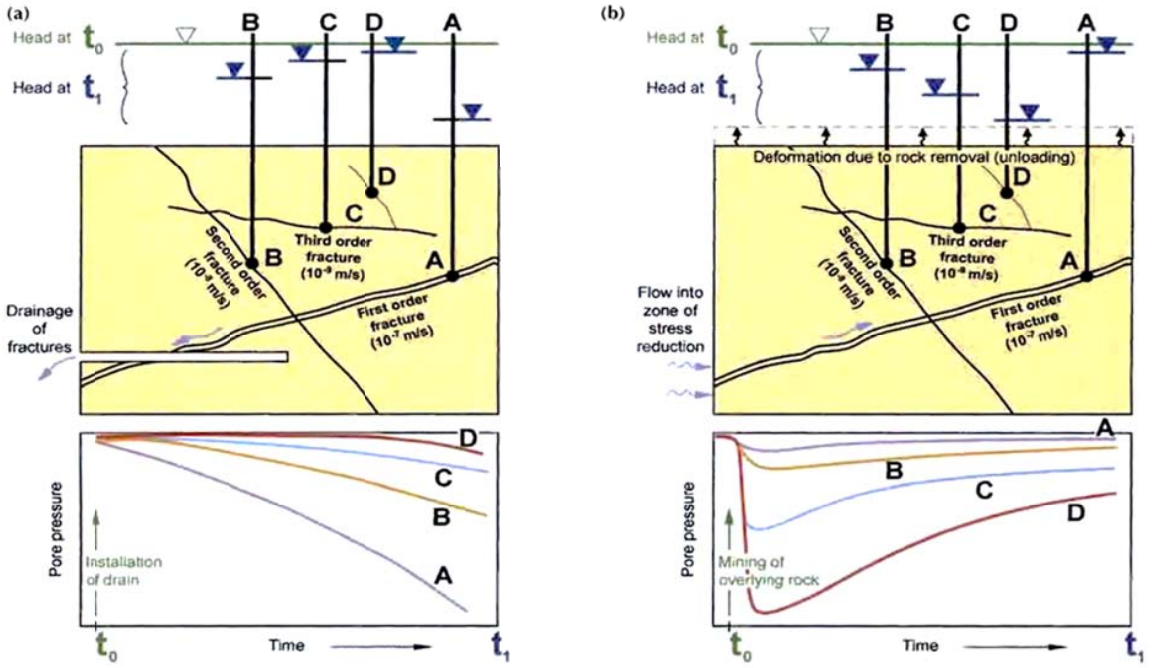

Fig. 1 Fractured controlled dual porosity (a) drainage response due to groundwater flow, (b) unloading response in a fractured rock mass [11]

B. Incorporation of Intact Rock Bridges

Methods for incorporating rock bridges into slope stability analysis can be divided into two categories [12], [13].

1. In-Plane Rock Bridges

Represented by conceptual patches of intact rock along a theoretical, fully-persistent discontinuity plane or failure surface. Jennings [14] proposes a method for incorporating the strength benefit of rock bridges on a candidate slope failure surface. Most recently, researchers have mapped in-plane rock bridges [15] on failure surfaces and on past rockfalls and wedge failures.

2. Out-of-Plane Rock Bridges

Out-of-plane rock bridges occur where discontinuities are non-coplanar. Usually out-of-plane rock bridges represent the shortest distance of intact rock between discontinuity tips. Nevertheless, this assumed rock bridge geometry may not always accurately predict the path of crack growth during slope deformation.

II. Numerical Modeling Approach

Improvements in computing technology have facilitated the development of increasingly sophisticated slope stability codes. This paper presents the simulation of a biplanar rock slope failure based on a theoretical wall section of an open pit.

The influence of varying percentages of rock bridges along the basal surface defining the biplanar failure mode is studied. Intact rock material, representing rock bridges was changed, in both size and location. Models considered the incorporation of explicit discrete fractures whose size, location and orientation were pre-determined and incorporated into the Slope Model code using the DFN embedded capability. Slope Model is a three dimensional brittle fracture code, that was develop as part of the Large Open Pit (LOP) project. The code uses an explicit solution scheme suitable for simulation of highly nonlinear behavior, such as fracture slip and opening/closing of joints [16]. Lorig et al. [17] used Slope Model to simulate failure of intact rock bridges in high rock slopes.

In order to build on the two previous observations, a basal plane of variable length and dipping at 15 degrees was incorporated at the toe of the pit slope. The percentages of rock bridges considered in this research were 5, 10 and 15% respectively. The locations of the fractures introduced into the model are presented in Fig. 2. Groundwater and its interaction with the rock bridge failure is also modelled and analysed.

A. Modelling Sequence

The models presented are for a semi-coupled hydro-mechanical analysis using the lattice spring scheme Slope Model code [16], and followed these steps (Fig. 3):

a) The first cycle involves initial flow calculations, allowing the initial pore pressure field determination.
b) Once a hydrostatic state is achieved, the second cycle corresponds to simulation of the mechanical model only, the rock bridges in-between the surfaces are broken through as a result of the induced stress.
c) Finally a third hydro-mechanical cycle is performed, where a newly formed flow pipe network is accounted for, and therefore, a new pore water pressure distribution is calculated.

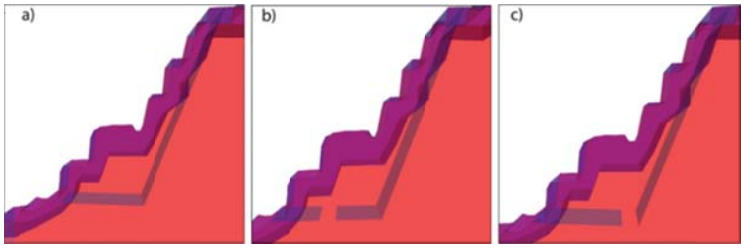

Fig. 2 Conceptual variation of the location of the modelled rock bridge percentages along the basal surface (a) at the daylighting end of the basal surface, (b) in the middle of the basal surface, and (c) at the inner end of the basal surface adjacent to the rear surface (The purple zone denotes the assumed blast damage extent)

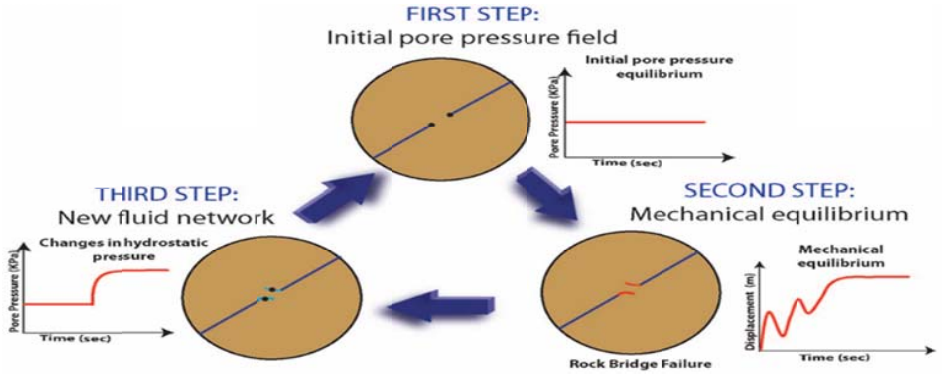

Fig. 3 Methodology and graphs showing the result of using different steps to analyze rock bridge failure in Slope Model [16], and typical results: Black dots represent history points

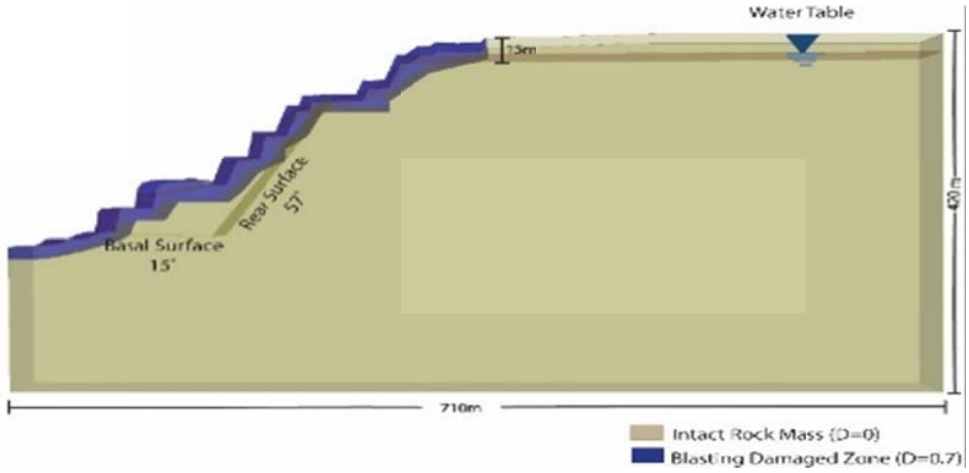

Fig. 4 Geometry used to simulate a biplanar failure mode in the Slope Model code

B. Slope Model Input Parameters

The general geometry is based on a mine case study and represents an open pit of 420 m in height with bench heights of approximately 30m. An assumed biplanar overall slope-scale failure including a rear surface dipping parallel to the slope at 57° and a basal surface dipping out of the slope at an angle of 15° was simulated. A non-manifold triangular surface representing the outer skin and internal surfaces of the model can be imported into the Slope Model code; where, internal boundaries are considered to be boundaries between materials, faults, etc. This model corresponds to a two-dimensional model extruded 40m out of plane. Outer surfaces correspond to the mechanical boundary conditions imposed as initial conditions for the model. The sides of the model are fixed such that horizontal displacements are constrained to zero; in the same way, the bottom of the model is fixed to ensure that no vertical displacements occur. The slope surface is free to move. The model geometry is shown in Fig. 4.

C. Rock Mass Properties

The rock mass properties used are based on the rock mass strength parameters presented in Table I.

TABLE I
ROCK MASS PROPERTIES USED IN THE SLOPE MODEL CODE

Property (Granite)	Value
GSI	75
Blast damage, D	0
Density (Kg/m^3)	2650
Young's modulus (GPa)	46
Poisson's ratio	0.25
UCS (MPa)	133
Tensile strength (MPa)	3.8
Friction angle (°)	57
Cohesion (MPa)	6
Porosity (%)	2
Permeability (m2)	5.7e-9 [19]

TABLE II
PROPERTIES USED FOR THE BLAST DAMAGE ZONE

Property	Value
GSI	75
Blast damaged	0.7
Density (Kg/m3)	2650
Young's modulus (GPa)	23
Poisson ratio	0.25
UCS (MPa)	133
Tensile strength (MPa)	3.4
Friction angle (°)	54
Cohesion (MPa)	5
Porosity (%)	2
Permeability (m2)	5.7e-4 [19]

Given the effect of mining activities on the surface of the slopes forming the pit, the model presented includes an assumed blast damaged zone. According to the guidelines provided by [18], a blast damage factor or D factor, should be considered when calculating the Hoek-Brown rock mass strength for the blast damaged zone. This parameter downgrades the rock mass strength, to allow for damage caused by blasting and slope dilation during mining activities. A factor D = 0.7 was used to account for the blasting effects caused on the pit walls. Additionally, the thickness of the blast damaged zone according to [18] should be taken into consideration. For this specific case, corresponding to a controlled blasting design; the thickness of this zone corresponds to half the overall bench height. A blasting damaged zone of 15m was therefore assumed parallel to the slope surface, corresponding to a T= 0.3 to 0.5H; where T is the thickness of damaged zone and H corresponds to the overall bench height, which in the case of the simulated open pit wall is 30m. Properties for models assuming a D = 0.7 for the blasting damaged zone are as stated in Table II.

D. Discontinuity Input Parameters

Discontinuities in the model were inserted by defining a continuous surface for the rear plane with a dip angle of 57°, with the mechanical properties shown in Table III. A basal surface with a dip angle of 15°, along which the rock bridges were considered, was also defined using the properties in Table III.

TABLE III
BASAL AND REAR SURFACE PROPERTIES USED IN SLOPE MODEL

Property	Basal Surface	Rear Surface
Tensile strength (MPa)	0	0
Friction angle (^{o})	42	25
Cohesion (kPa)	25	0
Kn (GPa/m)	8	4
Ks (GPa/m)	0.8	0.4

E. Slope Model Results

The base case model (Fig. 5) considered the simulation of fully persistent structures defining the rear and basal surfaces of the assumed biplanar failure mode. Since no preexisting discontinuities are incorporated within the sliding volume, rock mass dilation must occur entirely through brittle failure of lattice springs. Results indicate the creation of 120 cracks in the model in which a dry slope was assumed, mostly located towards the toe of the cross-section considered. Once groundwater is incorporated in the model, a slightly greater concentration of cracks is observed in the higher benches of the pit, within the blast damaged zone.

Figs. 6 and 7 show, respectively, the initial pore pressures and horizontal displacements for the different locations along the planes defining the rear and basal surfaces of the biplanar geometry.

Following the mechanical stage of the model, new displacements and cracking result in updating of the flow pipe network and hence, new pore water pressures are calculated at the points located along the basal and rear surfaces of the model. New fractures are created after 3 mechanical seconds of simulation (Fig. 8) and the pore pressures change for the points located on the rear (2 and 3) and on the basal surface (4), with the exception of point 1 which remains zero throughout the simulation time, as it is coincident with the location of the water table at the surface.

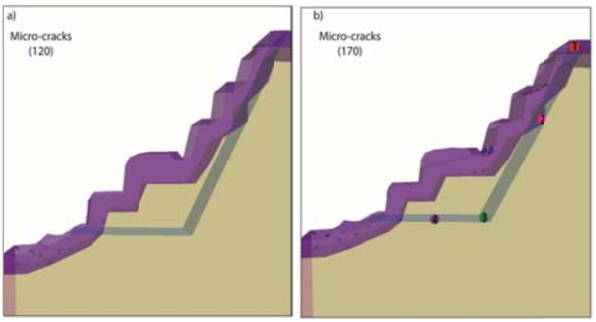

Fig. 5 Biplanar geometry and formation of cracks (represented by blue discs in the models), assuming continuous surfaces for the rear and basal surface (a) under dry conditions; (b) cracks developed for a model considering saturated conditions assuming a water table matching the slope profile. Coloured circles represent different location of history points, 1 and 2 along the basal surface, and 3 and 4 along the rear surfaces

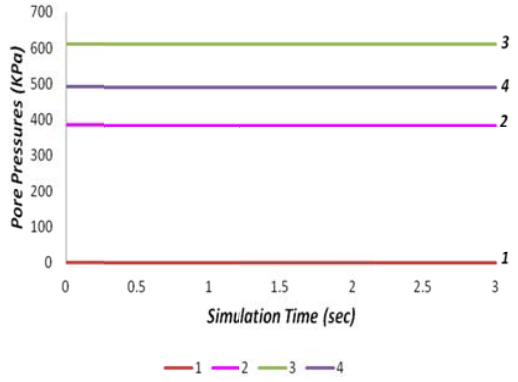

Fig. 6 Initial pore pressures assumed for a model considering continuous basal and rear surfaces. Location of history points is shown in Fig. 5

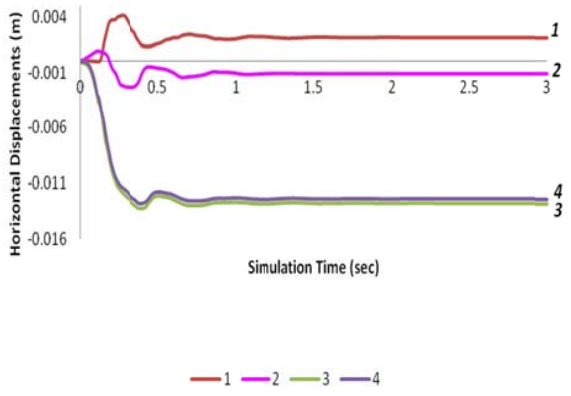

Fig. 7 Horizontal displacements for the history points located along the basal and rear surfaces (See Fig. 5)

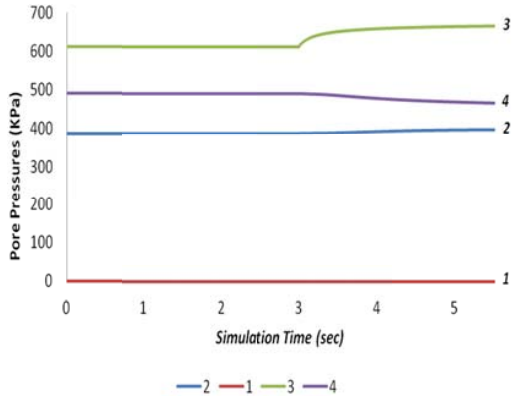

Fig. 8 Pore fluid pressures generated after new cracks are developed in the model

As the percentage of intact rock material (rock bridges) increases from 5 to 15%, results show that the numbers of fractures formed is, in general, greater for all simulated models where groundwater conditions are considered. Newly created fractures also increase as the intact rock material increases.

An exception takes place when the rock bridge is located at the inner tip of the basal plane in proximity to the rear surface; results show that the models develop a larger amount of fractures along the rear surface under dry conditions; an example of this behavior is presented in Fig. 9. The fracturing process tends to fracture part of the material representing the rear surface of the biplanar failure mode; possibly due to the low strength parameters representing this surface and the lack of pre-existing fractures in the sliding mass formed by the rear and basal surfaces, which increases the confinement effect in the sliding mass. Although, fewer new cracks are observed when groundwater conditions are considered in the model, the development of brittle fracturing is mainly confined to the areas along the basal surface where rock bridges were input.

When the rock bridge is located at the daylighting end of the basal surface in the proximity to the blast damaged zone, the models results show that many more micro-cracks are developed, particularly when considering groundwater conditions. This behavior may be linked to the blast damaged zone and that cracking increases the permeability and brittle behavior of the rock mass. The highest number of cracks occurs when the rock bridge is assumed to be located close to the rear surface.

Rock bridge failure along the basal surface generates changes in the distribution of pore pressures before and after breakage of intact rock material is achieved. Models considering a 5% rock bridge content result in total breakage of the intact rock material (Fig. 10), due to the influence of pore water pressures and therefore, new pore pressures are similar in magnitude and distribution to the base case model, which considers a fully continuous basal surface.

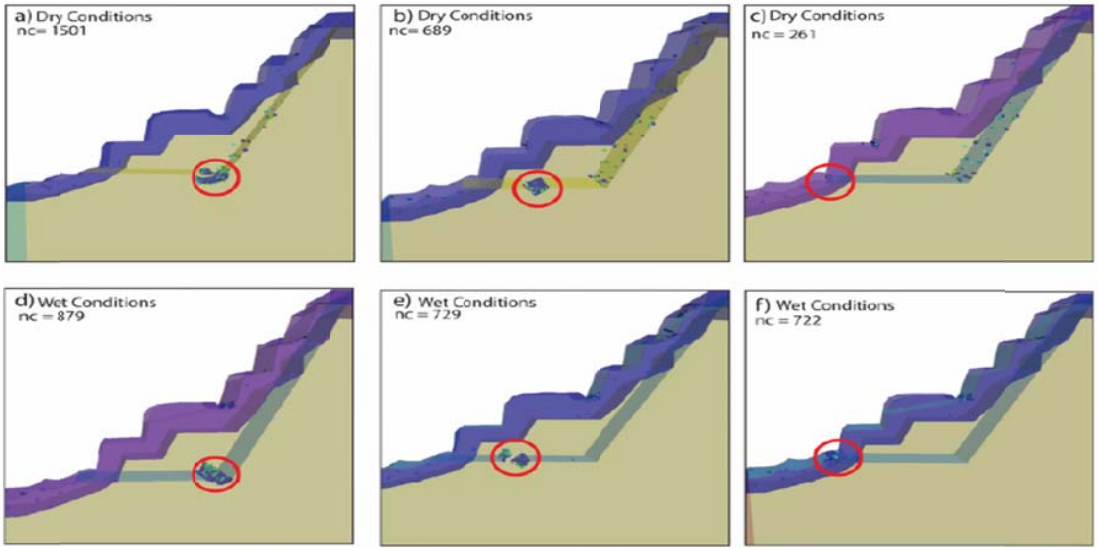

Fig. 9 Simulated failure for 15% rock bridge located at varying points in the slope enclosed in red circle (a) and (d) at the inner end of the basal surface; (b) and (e) at the middle of the basal surface; and (e) and (f) at the daylighting end of the basal surface under dry conditions (top) and considering groundwater (below): nc=number of cracks formed

When the rock bridge is increased to 10% and 15%, results show that the number of fractures formed is always greater for the models where groundwater conditions are considered. In contrast, when the rock bridge is located closer to the rear surface, dry models exhibit some random brittle behavior along the rear surface, which is no longer observed once groundwater is incorporated into the model. This may reflect the importance of reduction in effective shear strength along the rear plane. Similar results are achieved by models considering 10 and 15% rock bridges, full breakage of intact rock material does not occur. Results for a 15% rock bridge located at the end of the basal surface near the slope toe (Fig. 11), indicate that although there is intact rock breakage, the pore pressures generate by assuming a water table matching the slope profile are insufficient to entirely break through the rock bridge. Therefore, a wing crack develops at the tip of the discontinuity defining the basal surface.

When the rock bridge is located close to the rear plane (Fig. 12), fracturing occur primarily through the formation of wing cracks at the inner tip of the predefined discontinuities forming the basal and rear surfaces. Secondary cracks are seen to develop enclosing the area where the rock bridge was predefined. Pore pressures will eventually increase and stabilize at similar values. However, for the new fractures created within the intact rock material, the pore pressures do not appear to increase at the same rate with new fracture formation. This indicates a lack of connectivity for the basal surface

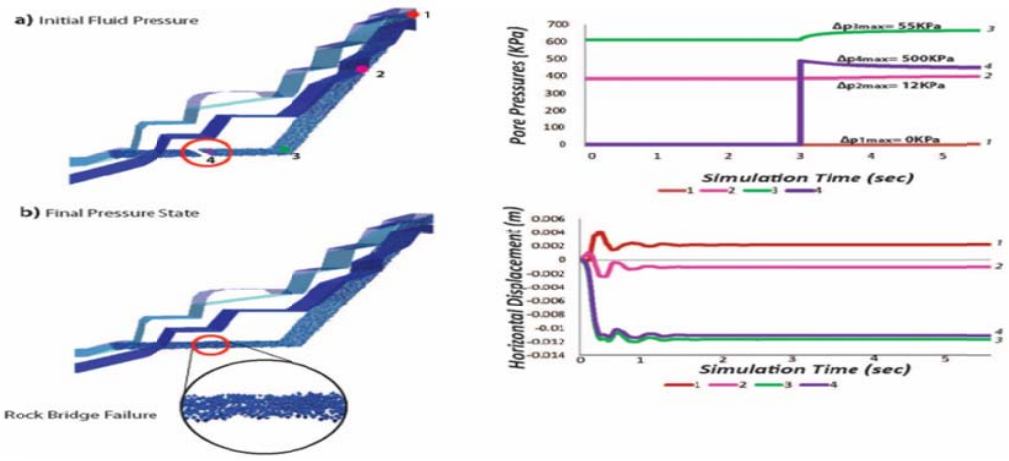

Fig. 10 Fracture pattern and pore pressure distributions before and after breakage of rock bridges induced by groundwater pressures. Considered a 5% rock bridge located at the middle of the basal surface. (a) Initial fluid pressure conditions (b) Final pressure conditions after new fractures have been created. Note lack of cracks connectivity. Plots of pore pressure and horizontal displacement for history points are presented on the right

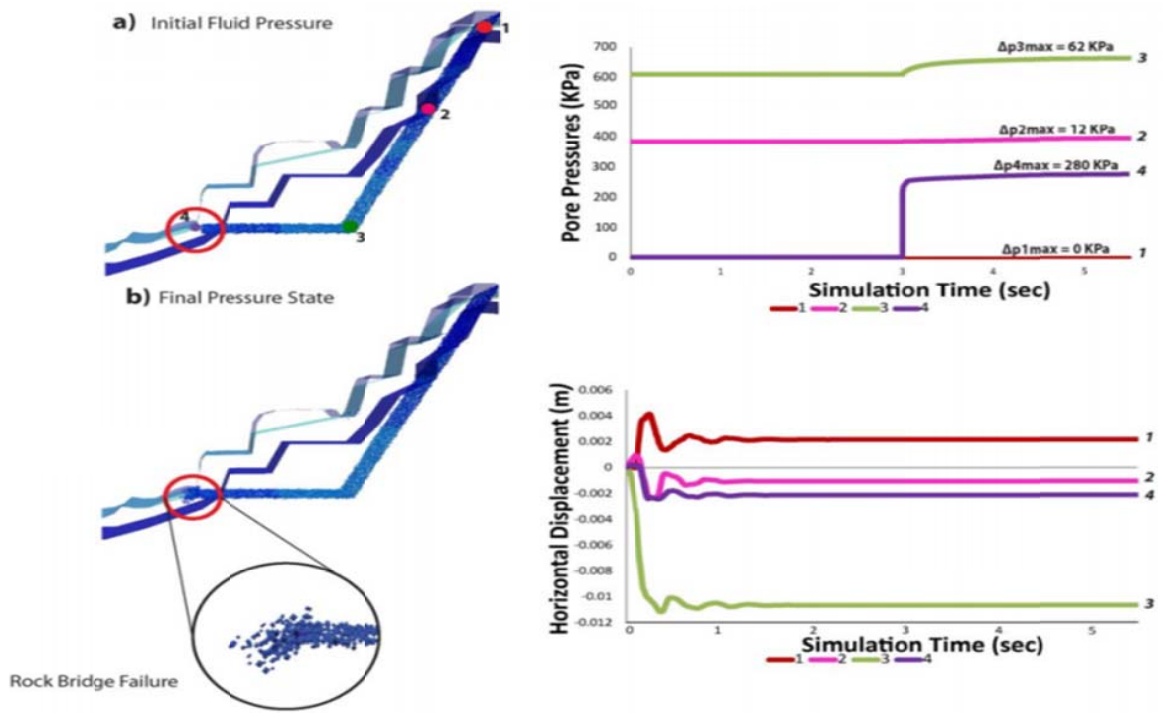

Fig. 11 Fracture pattern and pore pressure distributions before and after breakage of rock bridges induced by groundwater pressures. Considered a 15% rock bridge located at the daylighting end of the basal surface. (a) Initial fluid pressure conditions (b) Final pressure conditions after new fractures have been created. Note lack of crack connectivity. Plots of pore pressure and horizontal displacement for history points are presented on the right

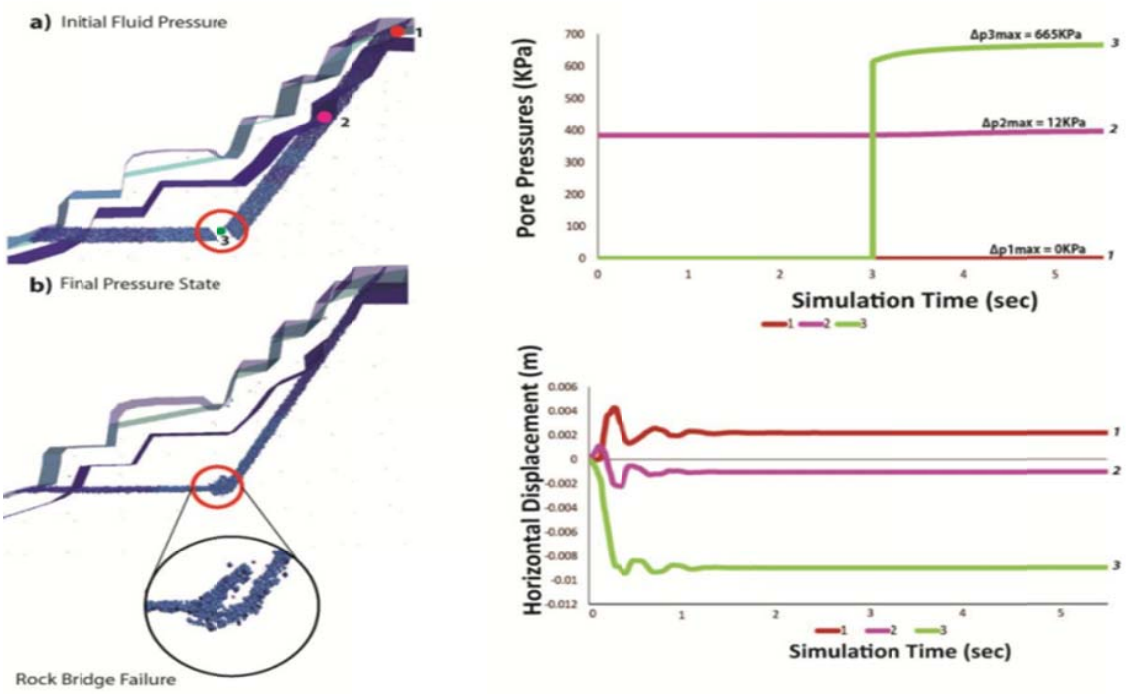

Fig. 12 Fracture pattern and pore pressure distributions before and after breakage of rock bridges induced by groundwater pressures. Considered a 15% rock bridge located close to the rear plane. (a) Initial fluid pressure conditions (b) Final pressure conditions after new fractures have been created. Note lack of crack connectivity. Plots of pore pressure and horizontal displacement for history points are presented on the right

Models assuming a rock bridge (10 and 15%) located at the middle of the basal surface (Fig. 13), show that although pore water pressures result in intact rock breakage, the cracks cannot fully interconnect along the basal surface, and as a result different pore pressure values are found at the two inner tips of the plane. Pore pressures cause local tensile stresses at the crack tips. In order for the fractures to grow, these newly formed fractures curve and develop into wing cracks, with marked differences in pore pressures at the tips of the discontinuities representing the basal surface. History points located within the rock bridge, suggests a sudden increase in pore pressures immediately after the creation of new fractures (after 3 seconds of mechanical calculation). This result is linked to those fractures that are not fully connected to the discontinuity closer to the rear surface; whereas on the side of the plane closest to the slope surface a drop in pore pressure is observed.

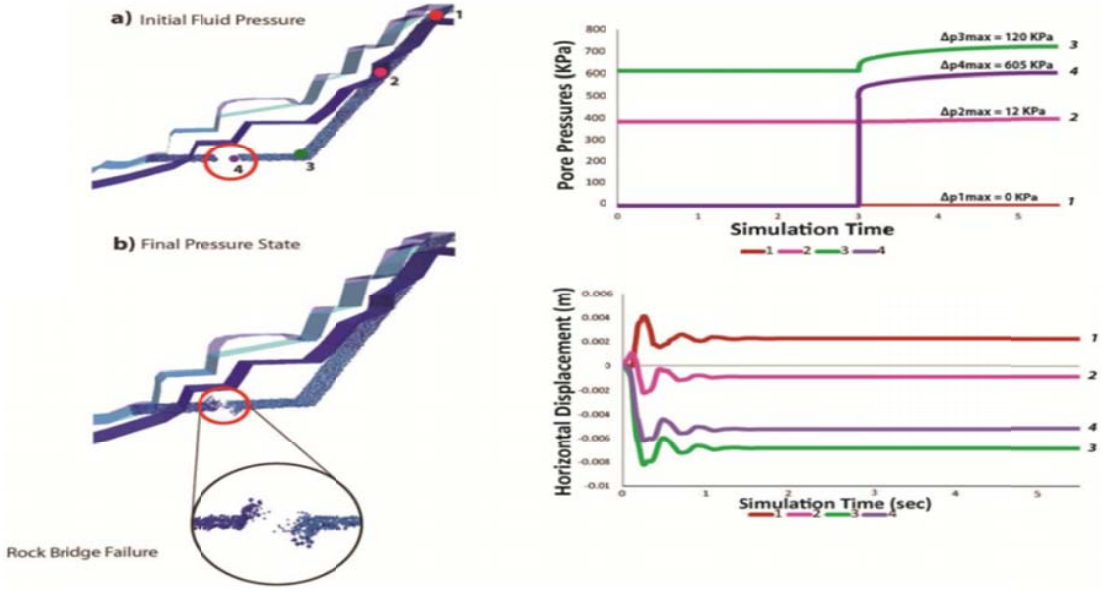

Fig. 13 Fracture pattern and pore pressure distributions before and after breakage of rock bridges induced by groundwater pressures. Considered a 15% rock bridge located at the middle of the basal surface. (a) Initial fluid pressure conditions (b) Final pressure conditions after new fractures have been created. Note lack of crack connectivity. Plots of pore pressure and horizontal displacement for history points are presented on the right

F. Summary of Results

The results presented in this paper demonstrate the effect of considering different percentages and locations of intact rock bridges along the basal surface comprising a biplanar failure mode. The effect of groundwater is shown through the number of cracks simulated in the Slope Model code. Different failure paths and changes in pore water pressures due to the rock bridge failure are observed and analyzed. According to the results of this research, the most critical case corresponds to a 5% rock bridge. Regardless of the location of an assumed 5% rock bridge, pore water pressures seem to be high enough to allow fractures to develop through the rock bridge creating a fully interconnected basal surface. When the percentage of rock bridges is increased to 10 or 15%, the failure pattern experienced by the rock involved in the rock bridge area changes, and fractures tends to fail in tension to form wing cracks and secondary cracks towards the tips of the discontinuities involved. The highest number of micro-cracks develops under dry conditions when the rock bridge is located at the inner tip of the basal surface. For this condition, cracks are formed along the rear plane, which slides and generates a different failure pattern, compared to models with groundwater. Although, more fractures are created under dry conditions for this rock bridge location, once groundwater is input in the model, the number of cracks is closely linked and due to the breakage of rock bridges. For all other locations, a greater number of fractures are formed when the rock bridge breakage occurs as a consequence of the input of groundwater pressure. This is especially true for the case when the rock bridge is located at the outer tip of the basal surface in the proximity to the blast damage zone.

The results of this research show that although rock bridges are broken through once the intact material percentage increases (10 to 15%), there is no longer full connection of fractures along the basal surface, and as a result different pore pressures values are found at the two inner tips of the plane.

Simulated models show the creation of wing cracks at the inner tips of the predefined discontinuities defining the basal surface, followed by the formation of primary and secondary cracks occurring within the rock bridges. This is especially true for the case where the rock bridge is assumed to be located closer to the rear plane. Pore water pressures indicate that when the rock bridge is assumed to be at the inner tip of the basal plane in proximity to the rear surface, pore pressures

will eventually increase and stabilize at similar values.

The models presented in this paper showed the importance of considering the development of brittle fracture as a result of the incorporation of groundwater conditions in rock slope analysis. The newly developed lattice-spring Slope Model, is proven to be a useful means to assess the initiation and propagation of brittle fracturing due to the inclusion of pore water pressures.

Acknowledgment

The authors would like to thank the sponsors of the Large Open Pit, LOP, project for the opportunity to use the Slope Model code in their research. We would also like to thank John Read of CSIRO, Australia, for his assistance in the provision of the Slope Model code, as part of this research completed at Simon Fraser University. The authors would like to acknowledge support for software training through the Itasca Education Partnership Program. Loren Lorig, Branko Damjanac, Maurilio Torres and Varun are thanked for their continued technical support and advice. Finally, we acknowledge Sonia D'Ambra (Golder Associates) for providing the pit slope geometry and some of the rock properties used for this investigation.

References

[1] Read, J., Beale, G., 2014. Guidelines for Evaluating Water in Pit Slope Stability. CSIRO Publishing. Collingwood, Victoria, 510pp.
[2] Vivas, J. Groundwater Characterization and Modelling in Natural and Open Pit Rock Slopes. (M.Sc. Thesis), Simon Fraser University. Burnaby, BC, Canada.
[3] Sullivan, T. D., 2007. Hydromechanical coupling and pit slope movements." In: Slope Stability Proceedings of the International Symposium on Rock Stability in Open Pit Mining.
[4] Read, J., Stacey, P., 2009. Guidelines for Open Pit Slope Design. CSIRO Publishing. Collingwood, Victoria, 512pp.
[5] Taseko, 2012. Preliminary Pit Slope Design (No. VA101-266/27-1). Taseko Mines Limited Consulting, Vancouver, Canadá, 78 pp.
[6] Hoek, E., 2002a. Blasting damage in rock, RocScience, 8 pp. Available online: https://www.rocscience.com/hoek/references/H2002.pdf
[7] Robertson, A.M., 1970. The interpretation of geological factors for use in slope theory. Planning Open, in: Planning Open Pit Mines, Proceedings. Johannesburg, pp. 55–71.
[8] Diederichs, M.S., Kaiser, P.K., 1999. Tensile strength and abutment relaxation as failure control mechanisms in underground excavations. Int. J. Rock Mech. Min. Sci. Vol. 36, pp. 69–96. doi:10.1016/S0148-9062(98)00179-X.
[9] Saiang, D., Nordlund, E., 2008. Numerical study of the mechanical behaviour of the damaged rock mass around an underground excavation, in: 5th International Conference and Exhibition on Mass Mining. Presented at the International Conference & Exhibition on Mass Mining, Lulea, Sweden, pp. 803–813.
[10] Coates, D. F. and Brown, A., 1961. “Stability of slopes at mines”, The Canadian Mining and Metallurgical Bulletin.
[11] Beale, G., Read, J., 2014. Guidelines for Evaluating Water in Pit Slope Stability. CRC Press, Australia.616 pp.
[12] Havaej, M., Stead, D., Lorig, L., Vivas, J., 2012. Modelling rock bridge failure and brittle fracturing in large open pit rock slopes, in: ARMA 2012. Presented at the 46th US Rock Mechanics / Geomechanics Symposium held in Chicago, IL, USA,, American Rock Mechanics Association, Chicago, IL, USA. 9 pp.
[13] Havaej, M., Wolter, A., Stead, D., Tuckey, Z., Lorig, L., Eberhardt, E., 2013.Incorporating brittle fracture into three-dimensional modelling of rock slopes. In: Proceedings of the 2013 International Symposium on Slope Stability in Open Pit. Mining and Civil Engineering, Brisbane, Australia., pp. 625–638.
[14] Jennings J. E. (1970). A mathematical theory for the calculation of the stability of open cast mines. In Van Rensburg, P. (Eds.), Planning open pit mines: Proceedings of the Symposium on the Theoretical Background to the Planning of Open Pit Mines with Special Reference to Slope Stability (pp. 87-102). Johannesburg, Republic of South Africa: Balkema (A.A.)
[15] Tuckey, Z., 2012. An Integrated Field Mapping-Numerical Modelling Approach to Characterising Discontinuity Persistence and Intact Rock Bridges in Large Open Pit Slopes (M.Sc. Thesis). Simon Fraser University. Burnaby, BC, Canada.
[16] Itasca Consulting Group, Inc., 2014. Slope Model Manual. Minneapolis, USA.
[17] Lorig LJ, Cundall PA, Damjanac B, Emam S. A three-dimensional model for rock slopes based on micromechanics. In: Proceedings of the 44th US Rock Mech Symp 5th US-Can Rock Mech Symp; 2010.
[18] Hoek, E., 2012. Blast Damage Factor D. In: Technical note for RocNews, February 2, 2012, Winter 2012 Issue, RocScience, pp. 6-8. Available from: www.rocscience.com/assets/files/uploadss/8584.pdf
[19] Zhang, L., 2013. Aspects of rock permeability. Frontiers of Structural and Civil Engineering. Vol. 7, pp. 102–116. doi:10.1007/s11709-013-0201-2.